

Supplementary Materials for
**Neurodevelopmental defects in human cortical organoids with
N-acetylneuraminic acid synthase mutation**

Qian Bu *et al.*

Corresponding author: Xiaobo Cen, xbcen@scu.edu.cn

Sci. Adv. **9**, eadf2772 (2023)
DOI: 10.1126/sciadv.adf2772

The PDF file includes:

Figs. S1 to S17
Legends for tables S1 to S3
Legends for movies S1 and S2

Other Supplementary Material for this manuscript includes the following:

Tables S1 to S3
Movies S1 and S2

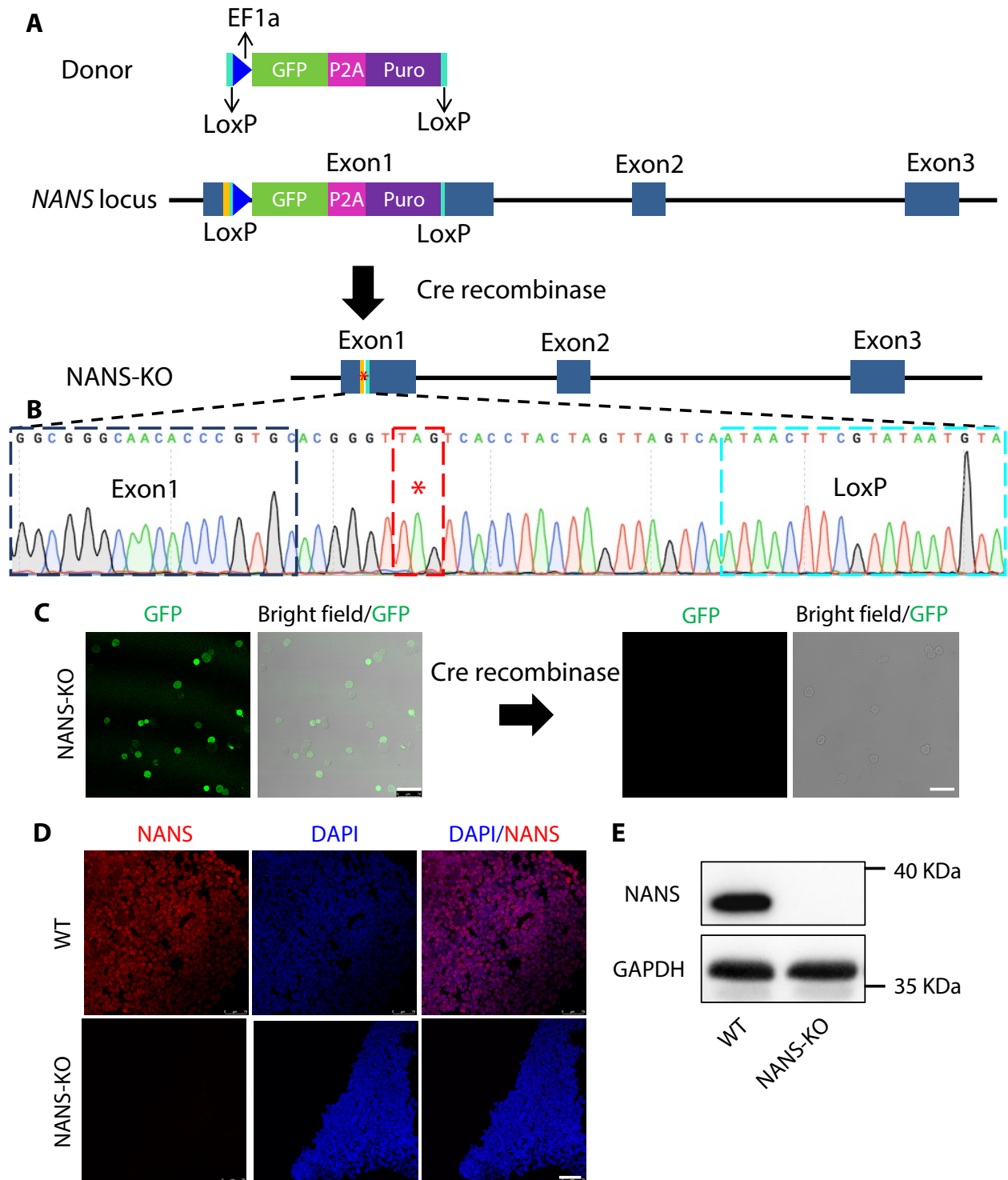


Figure S1. Generation of NANS-KO iPSC line without GFP expression.

(A) Schematic diagram of Cre recombinase-mediated deletion. Red star indicates an early stop codon.

(B) Representative sequencing chromatograms of DNA from NANS-KO iPSC line.

(C) NANS-KO iPSC line without GFP expression after Cre recombinase treatment. Scale bars: 75 μ m.

- (D) Confocal imaging of WT and NANS-KO iPSC lines after staining with antibodies against NANS. Scale bars: 75 μm .
- (E) Western blot analyses of NANS expression in WT and NANS-KO iPSC lines.

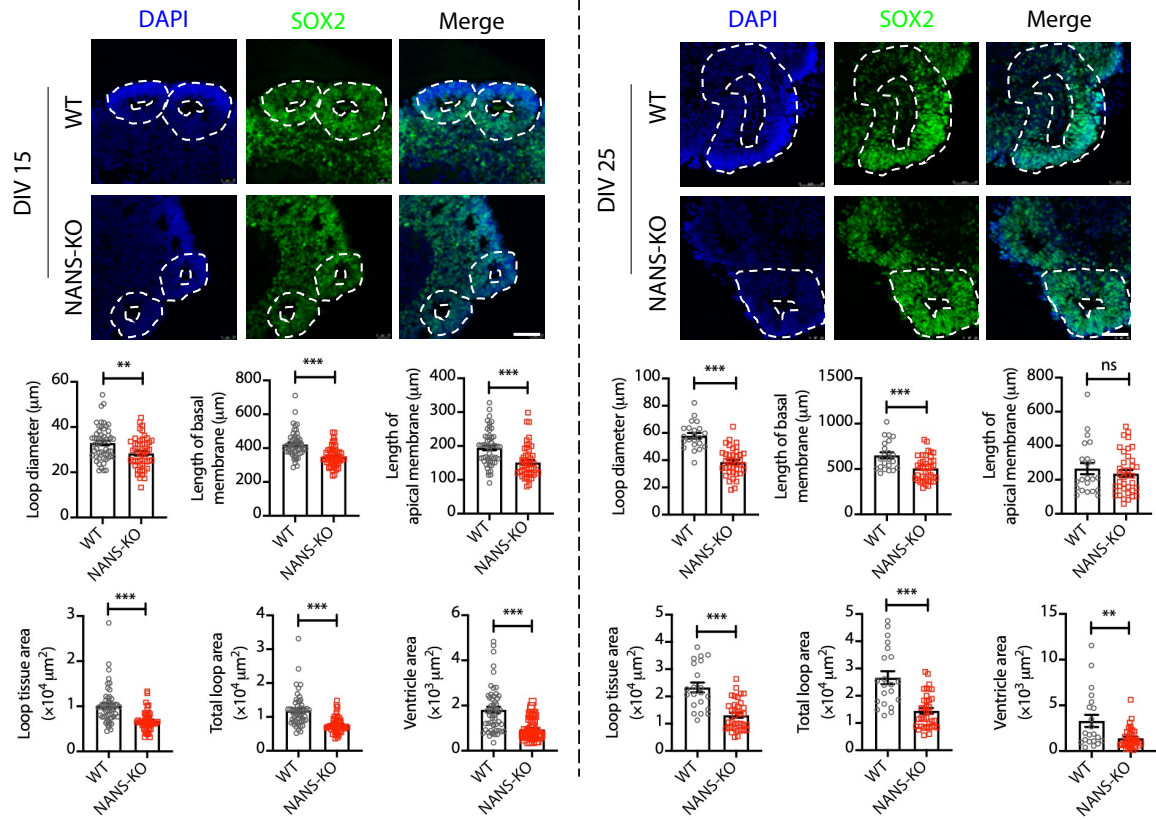


Figure S2. Representative images and the quantification of the VZ-like area in WT and NANS-KO cerebral organoids. n = 51~55 cortical structures (5~8 cortical structures per organoid) from 2 independent experiments at DIV 15; n = 22~38 cortical structures (4~6 cortical structures per organoid) from 2 independent experiments at DIV 25. ** $P < 0.01$; *** $P < 0.001$, Student's t -test. Scale bar: 50 μm .

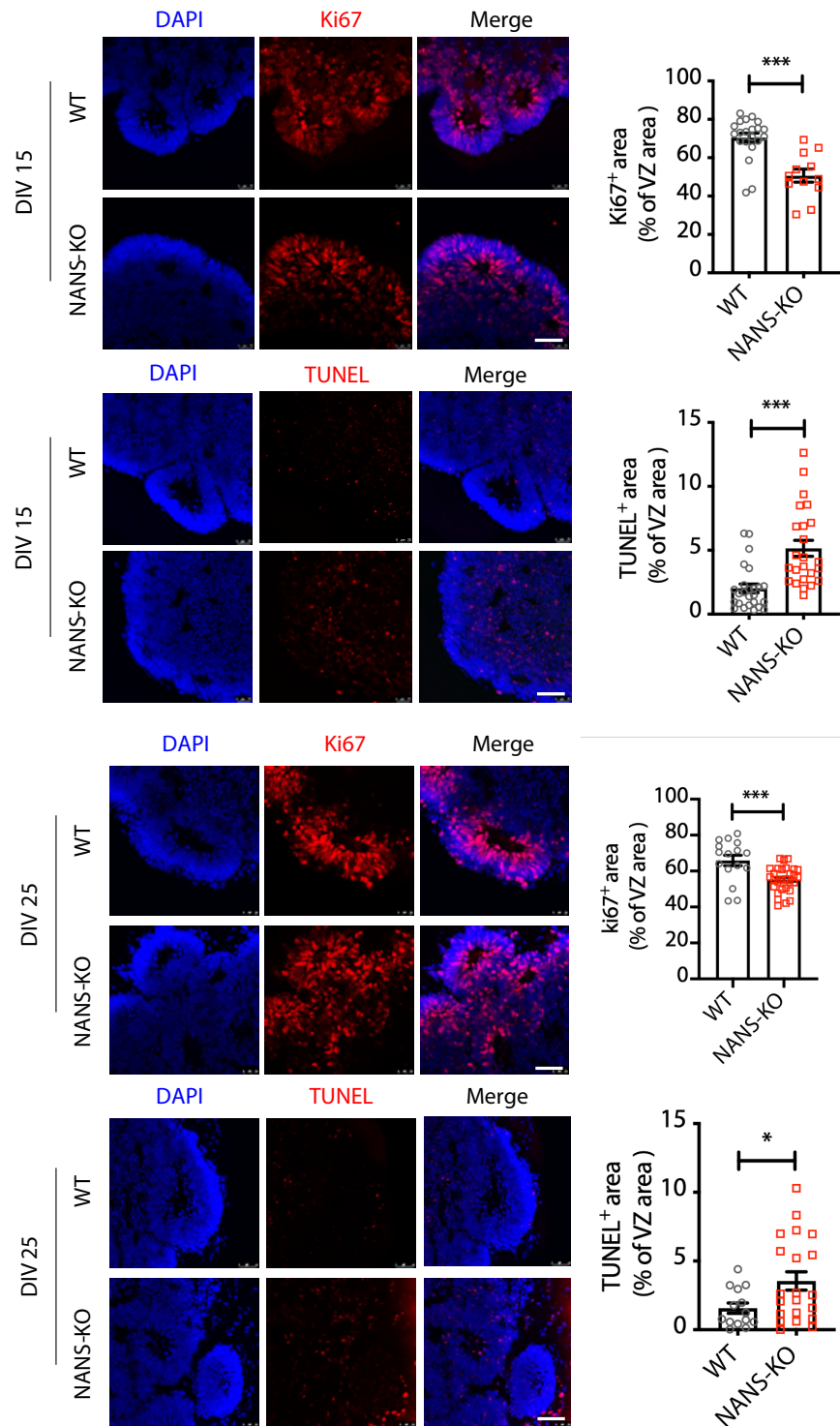


Figure S3. Representative images and quantification of WT and NANS-KO cerebral organoids stained with Ki67 and TUNEL. n = 12~21 cortical structures (4~7 cortical structures per organoid) from 1 independent experiment, * $P < 0.05$, *** $P < 0.001$, Student's t -test. Scale bar: 50 μm .

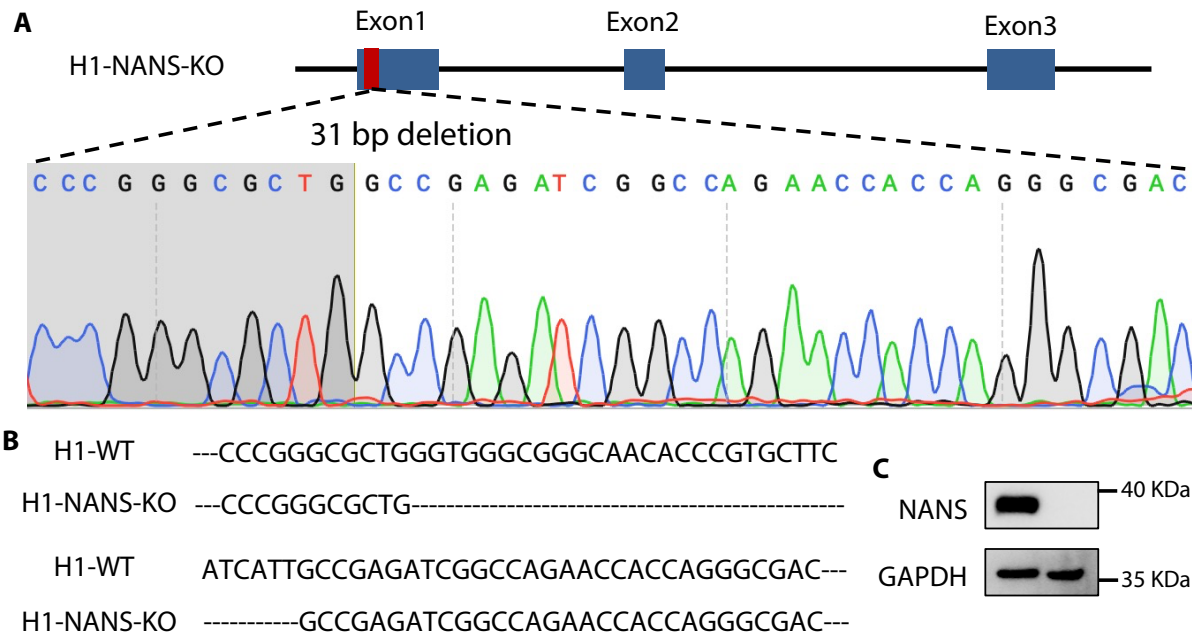


Figure S4. Generation of H1-NANS-KO hESC line.

- (A) Schematic diagram of the NANS knock-out strategy in H1 hESC line, and sanger sequencing.
- (B) Representative sequencing chromatograms of DNA from the H1-WT and H1-NANS-KO hESC lines.
- (C) Western blot analyses of NANS protein in H1-WT and H1-NANS-KO hESC lines.

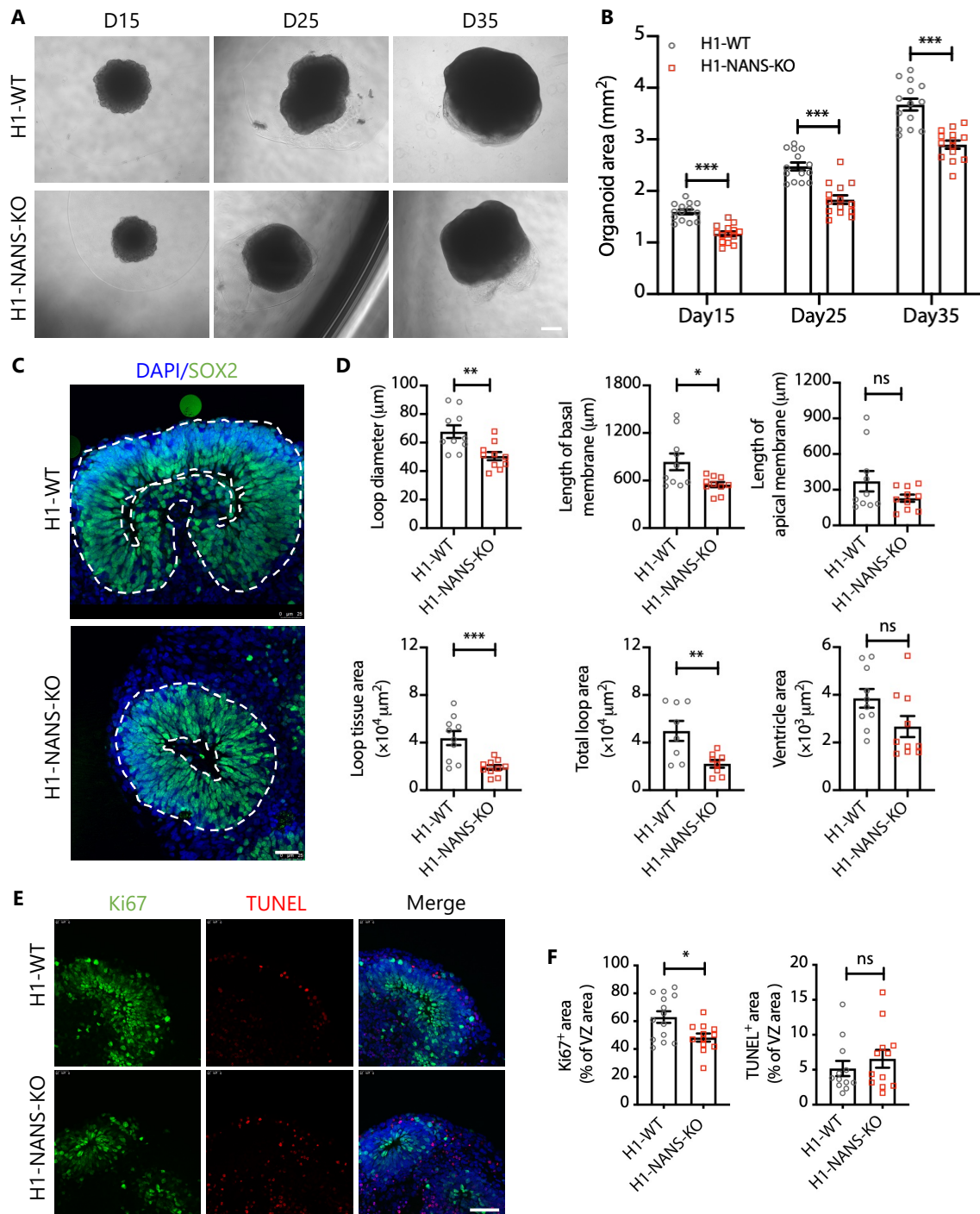


Figure S5. Reduced size and expansion of cerebral organoids in H1-NANS-KO cell line.

(A) Bright-field microscopy images of H1-WT and H1-NANS-KO cerebral organoids at DIV 15, 25, and 35. Scale bar: 500 μm .

(B) Quantification of cerebral organoid area. $n = 14$ organoids from 1 independent experiment.

*** $P < 0.001$, two-way repeated-measure ANOVA followed by Bonferroni's multiple comparisons test.

- (C) Confocal imaging H1-WT and H1-NANS-KO cerebral organoids at DIV 35 after staining with antibodies against SOX2. Scale bars: 75 μm .
- (D) Quantification of the parameters in the neuroepithelial loops of H1-WT and H1-NANS-KO cerebral organoids at DIV 35. $n = 10$ neuroepithelial loops (4~5 neuroepithelial loops per organoid) from 1 independent experiment, $*P < 0.05$, $**P < 0.01$, $***P < 0.001$ Student's t -test.
- (E) Representative images of H1-WT and H1-NANS-KO cerebral organoids at DIV 35 were stained with Ki67⁺ and TUNEL⁺. Scale bar: 50 μm .
- (F) Quantification of the percentage of Ki67⁺ and TUNEL⁺ positive cells among the total cells in the examined areas. $n = 12$ cortical structures (3~5 cortical structures per organoid) from 1 independent experiment, $***P < 0.001$, Student's t -test.

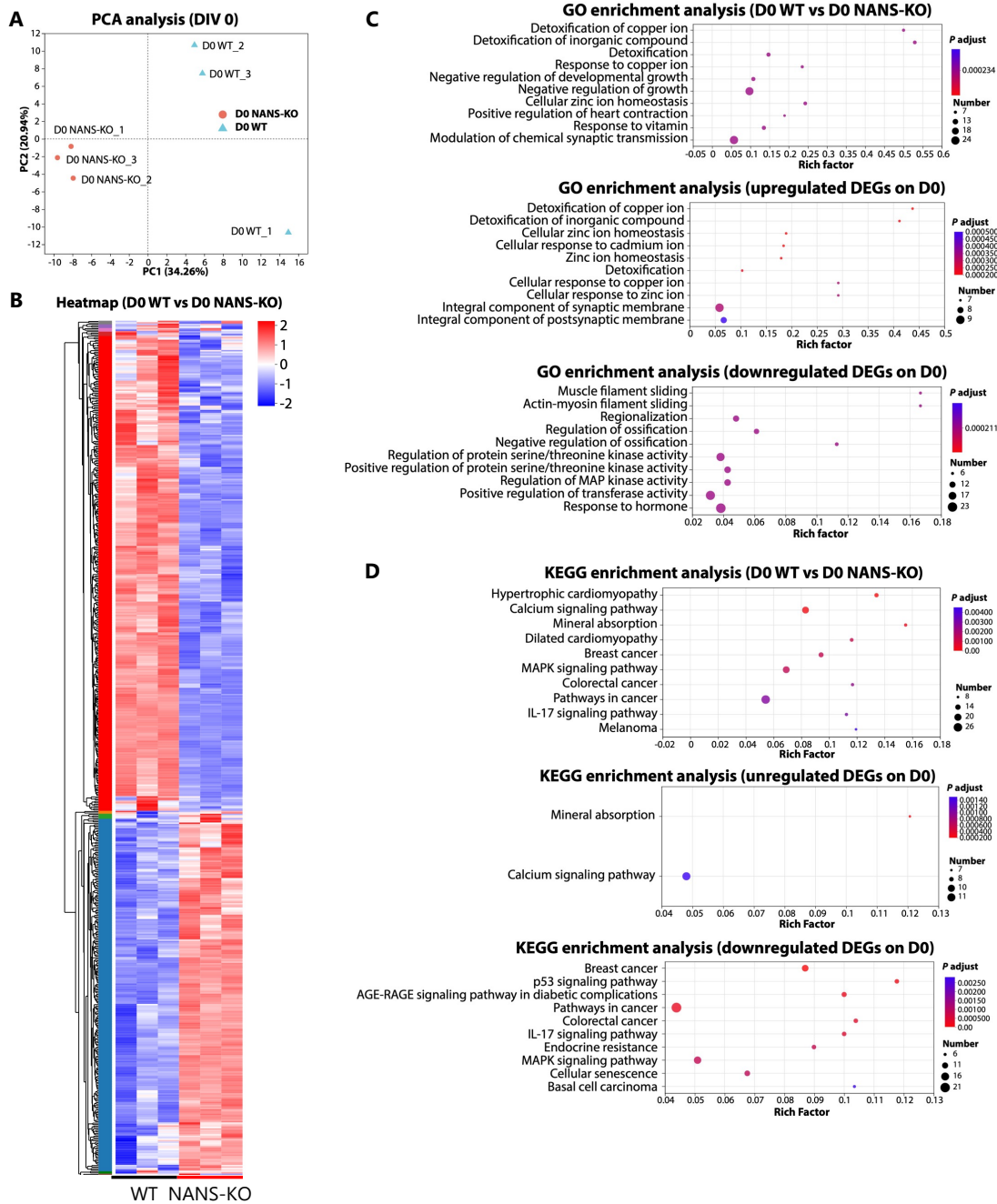


Figure S6. The PCA, heatmap, GO and KEGG enrichment analysis of DEGs in WT and NANS-KO iPSCs.

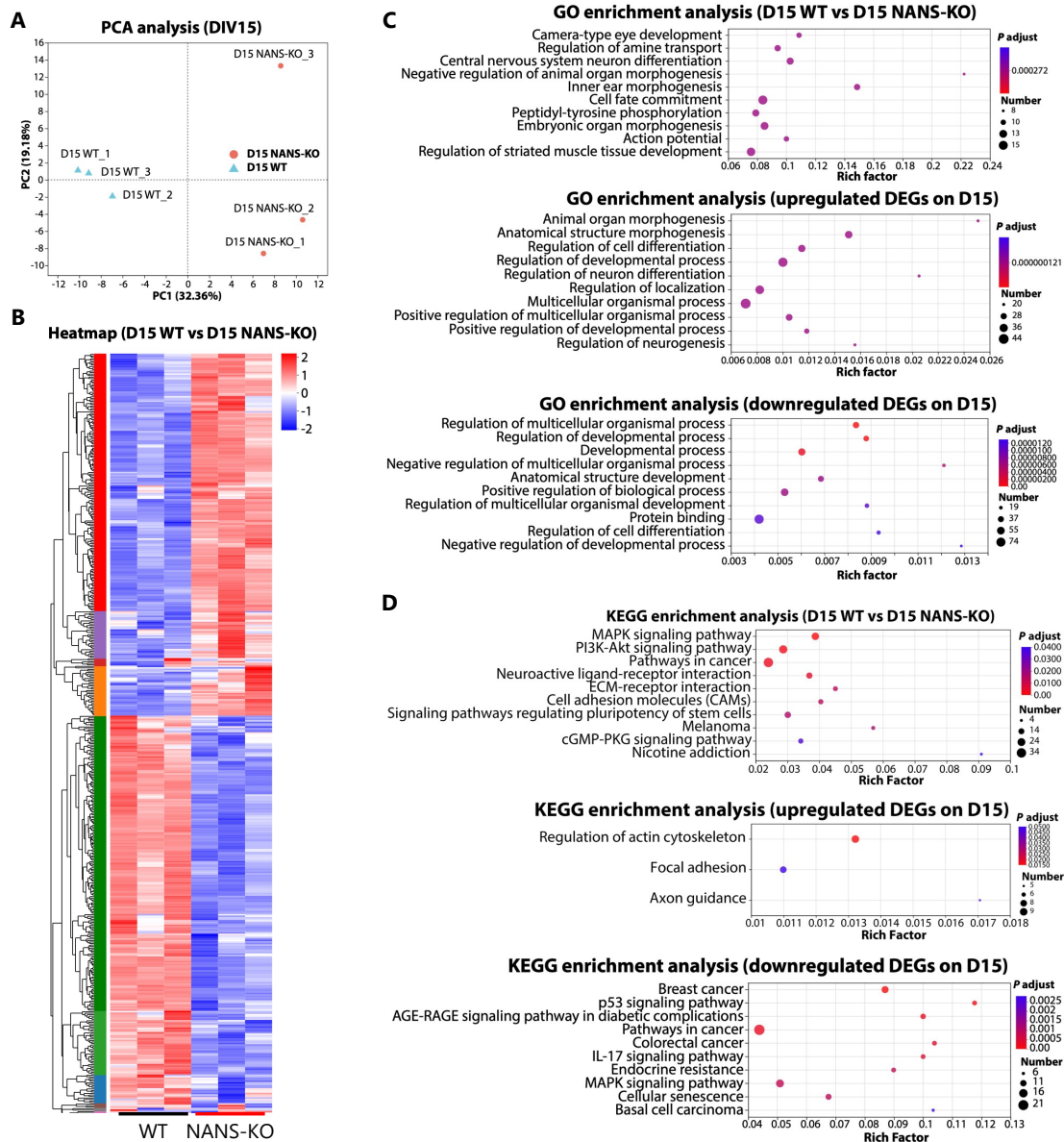


Figure S7. The PCA, heatmap, GO and KEGG enrichment analysis of DEGs in WT and NANS-KO cerebral organoids at DIV 15.

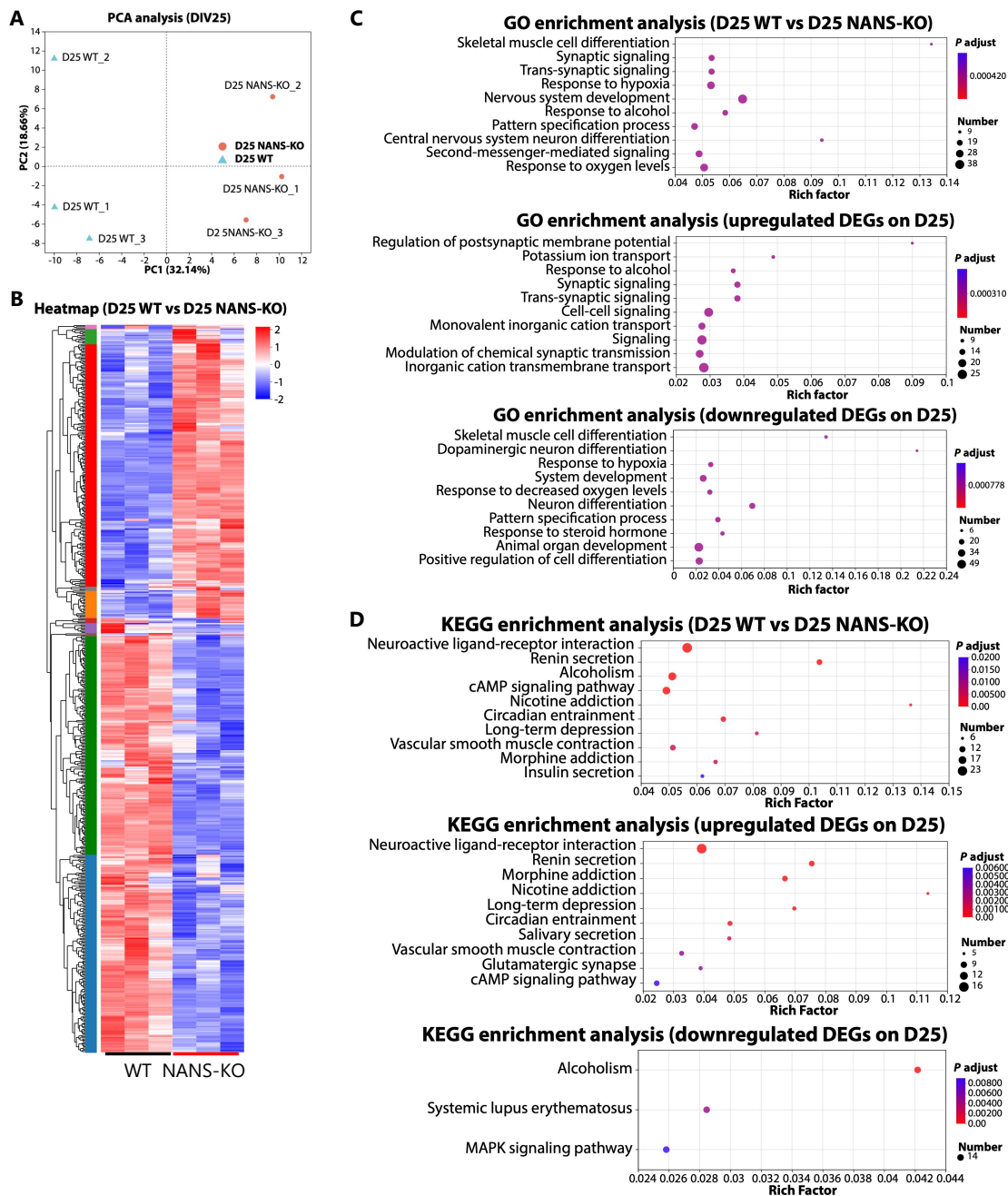


Figure S8. The PCA, heatmap, GO and KEGG enrichment analysis of DEGs in WT and NANS-KO cerebral organoids at DIV 25.

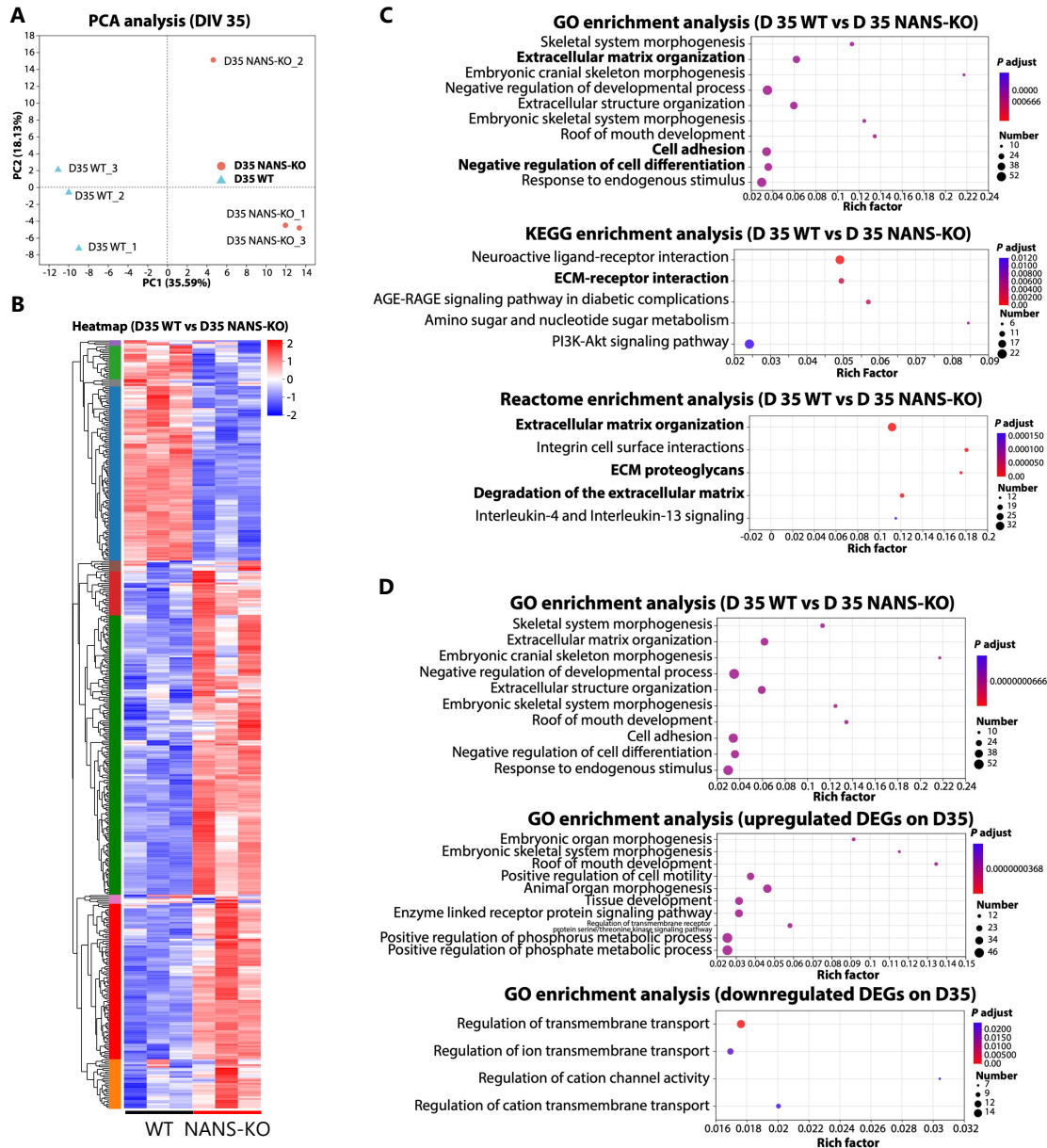


Figure S9. The PCA, heatmap, GO and KEGG enrichment analysis of DEGs in WT and NANS-KO cerebral organoids at DIV 35.

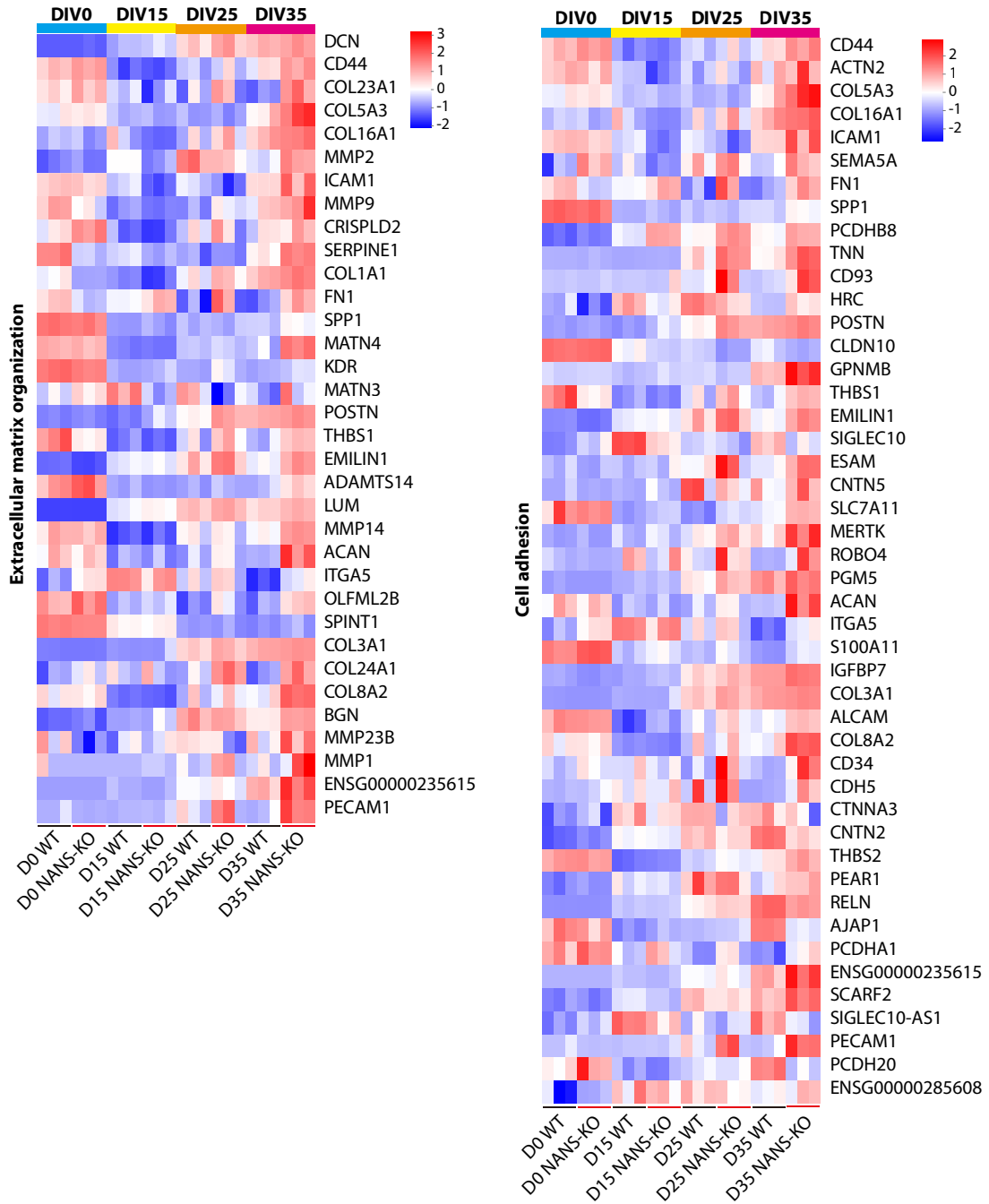


Figure S10. Gene expression heatmap of extracellular matrix organization and cell adhesion at DIV 0, 15, 25, and 35

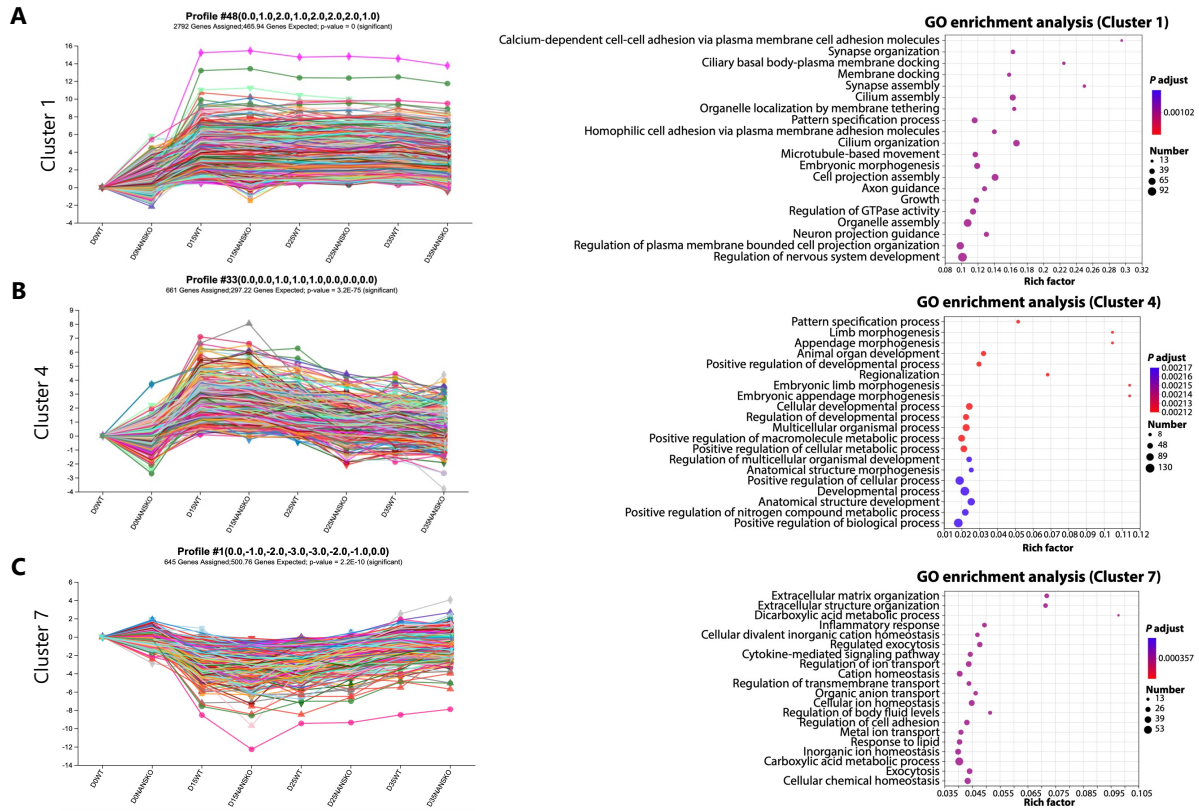


Figure S11. GO enrichment analysis of genes in cluster 1, 4 and 7.

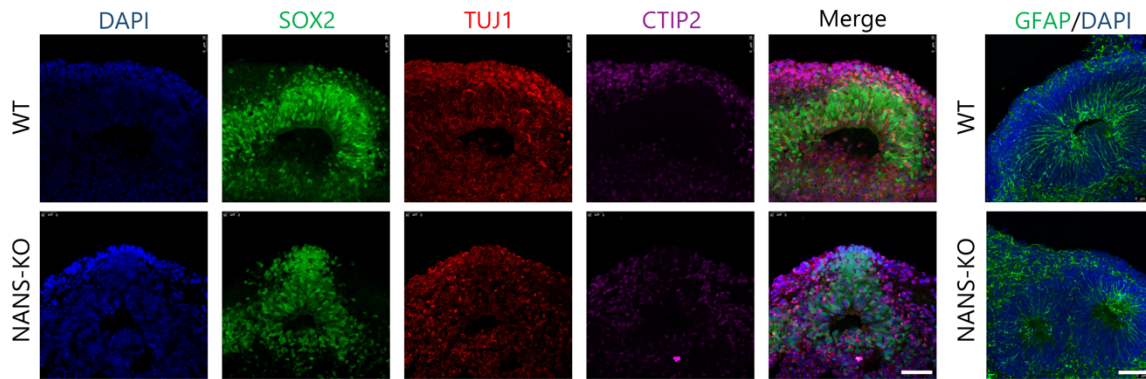


Figure S12. Characterization of cerebral organoids from WT and NANS-KO. Immunostaining of SOX2 (green), TUJ1 (red), CTIP2 (purple), and GFAP (green) in cerebral organoids at DIV 63. The cell nuclei were stained with DAPI (blue). Scale bar: 50 μm .

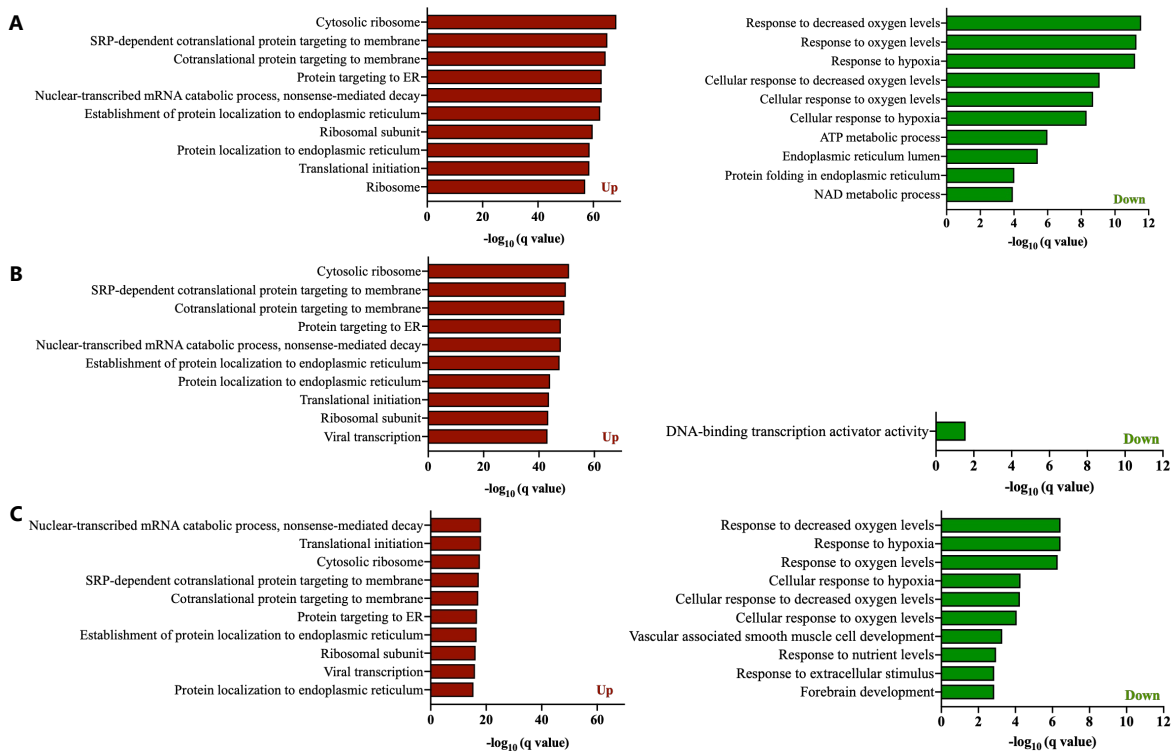


Figure S13. GO enrichment of glia (A), neuron (B), and oRGs (C) in cerebral organoids at DIV 63.

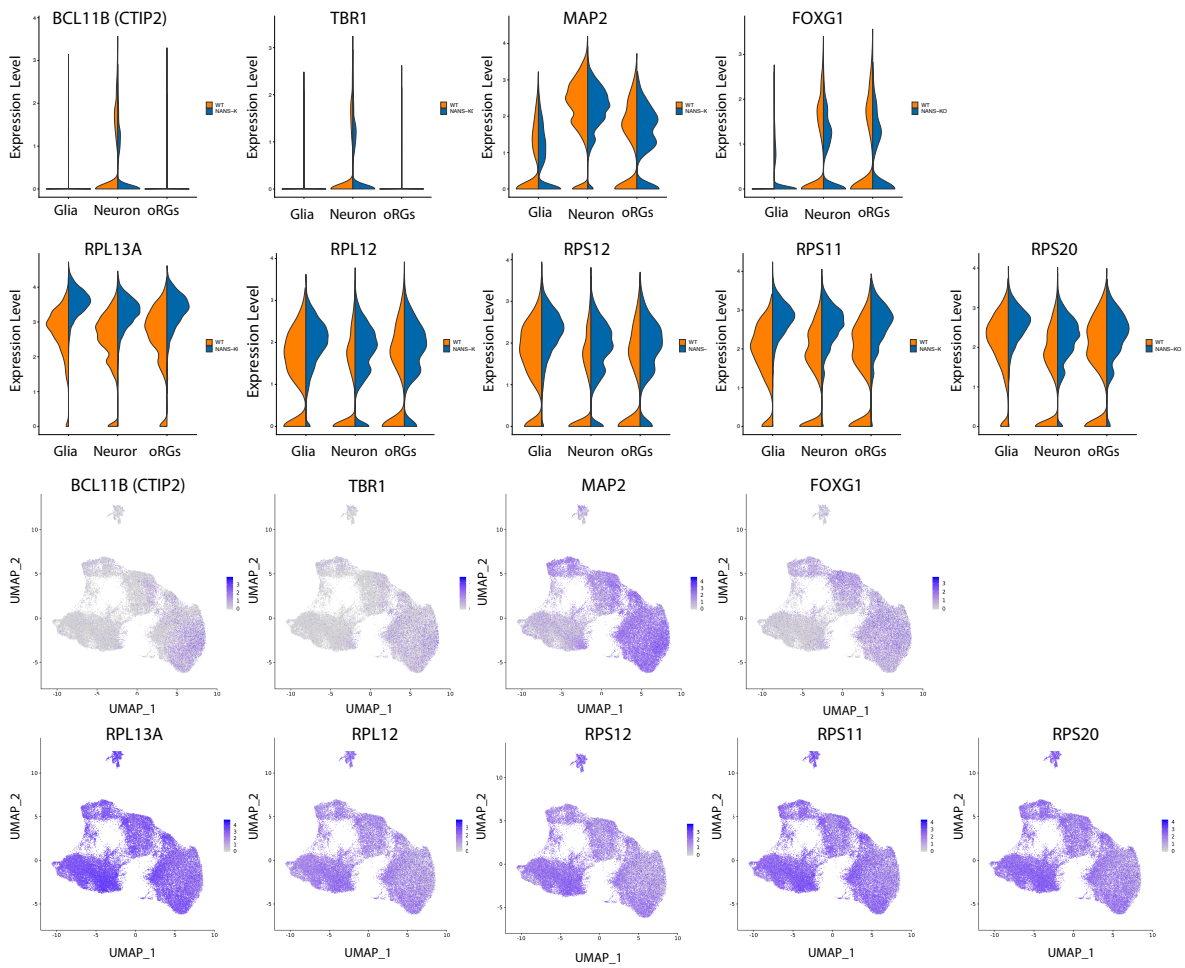


Figure S14. Violin plot and feature plots of BCL11B (CTIP2), TBR1, MAP2, FOXG1, RPL13A, RPL12, RPS12, RPS11, and RPS20 in WT and NANS-KO cerebral organoids.

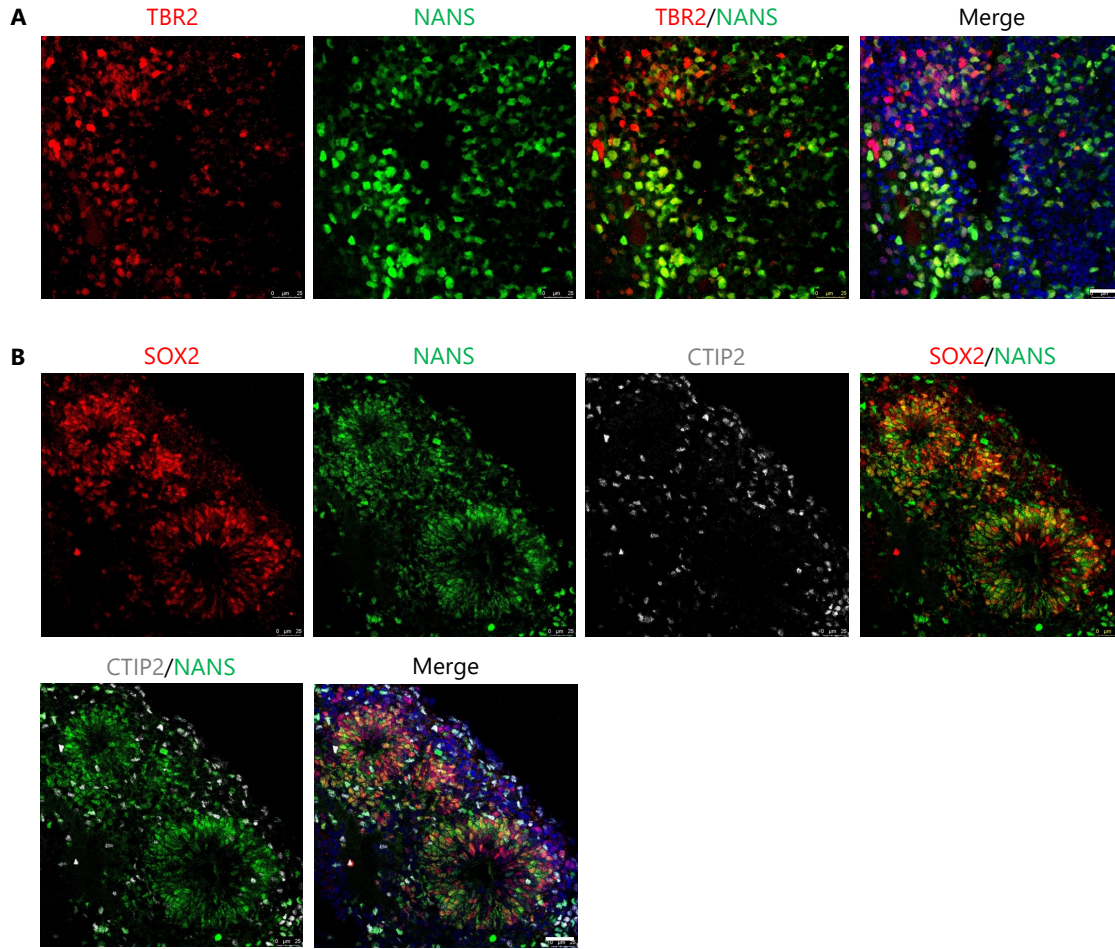


Figure S15. Immunostaining of TBR2/NANS (A) and SOX2/NANS/CTIP2 (B) in cerebral organoids at DIV 63. Cell nuclei were stained with DAPI (blue). Scale bar: 25 μ m.

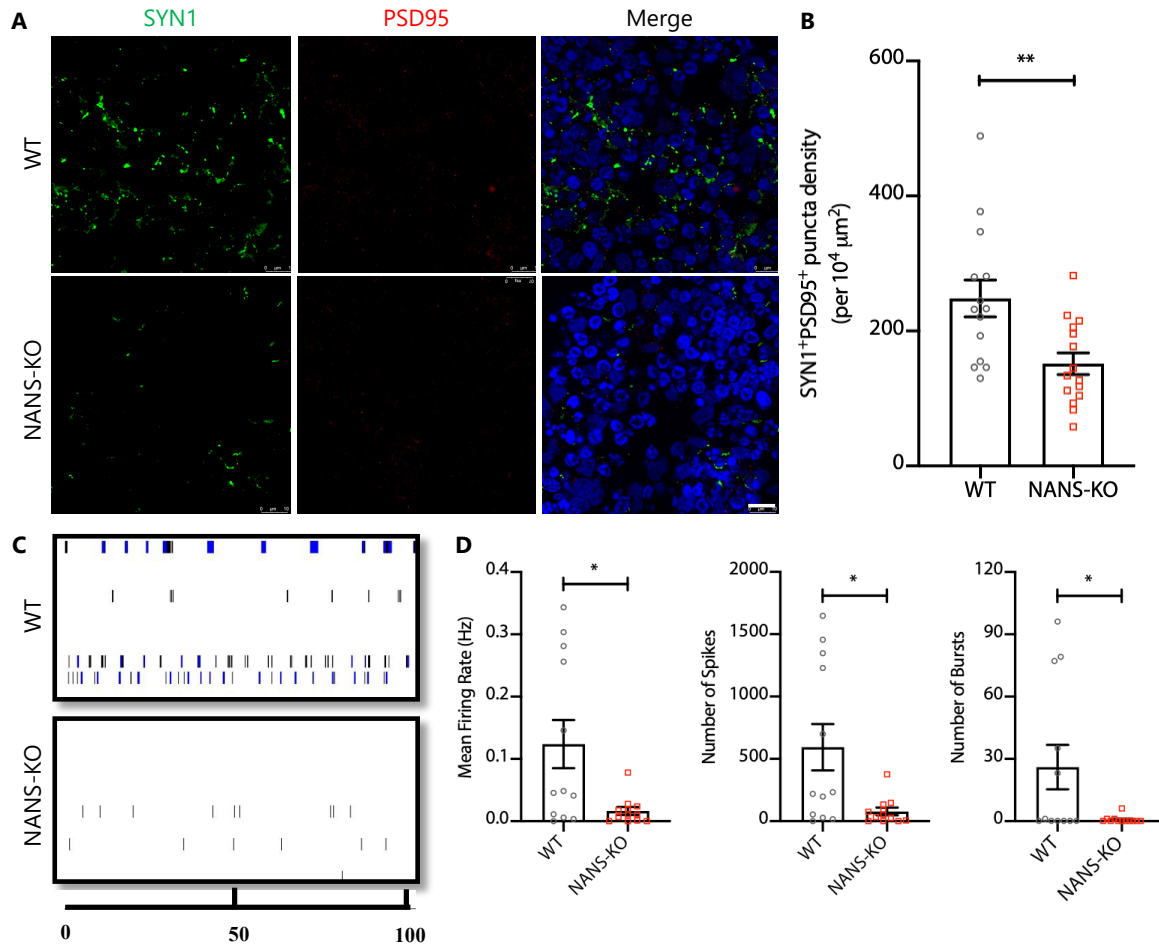


Figure S16. Additional functional characterizations of *NANS* mutation impairs synapse formation and neuronal network activity, related to Figure 6.

(A and B) *NANS* mutation impairs synapse formation in *NANS*-KO organoids. Representative images (A) and quantification (B) of SYN1⁺/PSD95⁺ puncta density in WT and *NANS*-KO cerebral organoids at DIV 63. $n = 14\sim 15$ cortical structures (3~5 cortical structures per organoid) from 2 independent experiments, $**P < 0.01$, Student's t-test. Scale bar: 10 μm.

(C) Representative spike raster plots of WT and *NANS*-KO-derived cortical neurons.

(D) MEA analysis reveals a reduction in the mean firing rate and the total number of spikes and bursts in *NANS*-KO neurons. $n = 12$ MEA wells per genotype from 1 independent experiment, $*P < 0.05$, Student's t-test.



B PCR screening
 Forward primer (F1): 5'-AACACCTACTTTCCTGACTGCTT-3'
 Reverse primer (R1): 5'-ACAATAGCACCTTGTCTGGGTTT-3'
 Targeted allele: 523 bp Wildtype allele: 14268 bp

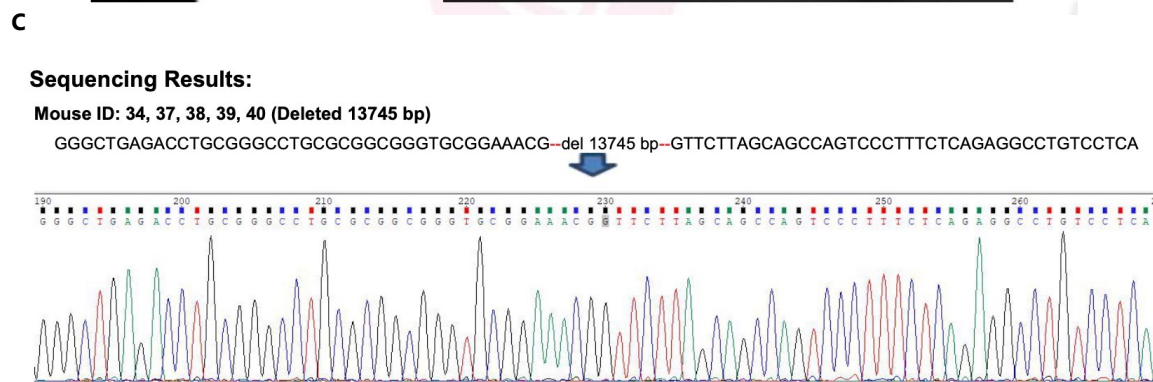
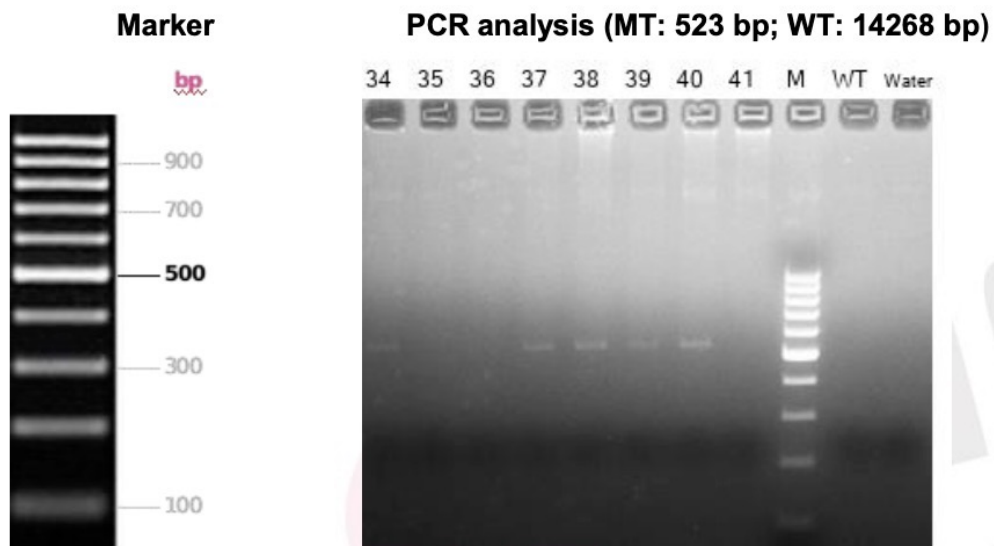


Figure S17. Generation and characterization of the *Nans*^{+/-} mice.

(A) Schematic diagram of the *Nans*^{+/-} targeting strategy in mice.

(B) PCR screening of *Nans* in mice.

(C) Representative sequencing chromatograms of DNA from the *Nans*^{+/-} mice, showing the 13745bp deletion in *Nans*^{+/-} mice.

Other Supplementary Materials for this manuscript include the following:

Supplementary Table S1. Biomarkers for neuronal cells.

Supplementary Table S2. RNA-seq - Differentially expressed genes in WT and NANS-KO cerebral organoids at DIV 0, 15, 25, and 35. Related to Figure 3.

Supplementary Table S3. Time-series clustering of the genes based on gene expression profile changes was conducted using the STEM software. Related to Figure 3

Supplementary Movie S1. Live imaging of WT migrating cortical neurons.

Supplementary Movie S2. Live imaging of NANK-KO migrating cortical neurons.